The Validation of Feeder Modeling for Ductile Iron Castings

Fu-Yuan Hsu and Yu-Hung Chen

Abstract A precise feeder design for a ductile iron casting is difficult, due to the complexities of its liquid–solid states transformation. During solidification, a negative pressure in castings is developed from the volumetric shrinkage as liquid iron solidified, while a positive pressure is added from the volumetric expansion as spheroidal graphite crystallized from the liquid iron. A unique crystalline structure of Austenite shell surrounds the spherical graphite and also increases the viscosity of feeding fluid flow. First principle model was applied for modeling the flow behavior of the residual liquid iron during solidification. The phenomenon of volumetric expansion as spheroidal graphite crystallized was also considered. The model was validated by real casting a cube-shaped cast. The predictions of the shrinkage area and porosities were confirmed by the hardness contours in the cross-sectional area of the castings. An optimized solidification modulus ratio of the feeder to this cube cast was suggested.

Keywords Ductile cast iron · Feeder design · Hot spot · Modeling validation · Spheroidal graphite

Introduction

In the Campbellology, spherical graphite was precipitated from liquid cast iron through various steps of the nodulation process in ductile cast iron [1]. Using 2.5-mm-alumina refractory tube drawing magnesium-treated ductile cast iron melt, Fredriksson et al. explore various directional solidification experiments and rapidly quenched the tube for metallographic analysis [2]. They found that the volume fraction of austenite in dendrites is about 10 times larger at the early stage of the

F.-Y. Hsu (✉) · Y.-H. Chen
Department of Materials Science and Engineering, National United University,
No. 1 Lein-Da, Kung-Ching Li, MiaoLi 36003, Taiwan, ROC
e-mail: willyhsu@nuu.edu.tw

M. Tiryakioğlu et al. (eds.), *Shape Casting*, The Minerals, Metals & Materials Series,
https://doi.org/10.1007/978-3-030-06034-3_22

solidification process (i.e., the solid fraction around 0.1 $\sim$ 0.2) comparing to those of austenite in shell and graphite spheroids.

In this earlier stage of ductile iron solidification, the volume fraction of graphite is less than the critical value of the gray iron solidification given by Schmidt et al. [3]. At this solidification time, volumetric shrinkage occurs because of the liquid transforming to a high density of austenite with a little (or less) low density of graphite. It could be easily compensated by filling in new liquid from a feeder or from parts of casting solidifying later. If no feeders are used, macro-pores will be formed.

In the solid fraction greater than 0.4, the precipitation of graphite nodule inside austenite shell then increases. Austenite shell will thus be plastically deformed dramatically, and these solid austenite grains coherently interact with each other to form networks. At this time, it is difficult to transport the melt through networks of austenite grains (e.g., mass feeding in five feeding mechanisms by Campbell [1]). Also, the melt scattered with the nodules becomes a highly viscous non-Newtonian fluid. The feeding efficiency of a feeder in a ductile iron casting is low, comparing to that in gray iron. The macro-pores will then remain, although some other parts of casting may be expanded overall due to the growing of graphite nodules at solid fraction greater than 0.4 $\sim$ 0.5. In later solidification (e.g., solid fraction above 0.67), the micro-pores are formed from the residual melt encapsulated within networks of austenite shells.

Therefore, the best method to locate macro-pores in a ductile iron casting is to track the level of its liquid region during solidification process. An accurate modeling package is required to predict exact locations of macro-pores in ductile iron castings.

Method

The freezing time of any solidifying body is approximately controlled by its own geometric modulus *(M)*, which is the ratio of its volume *(V)* over its cooling surface area *(A)*. The modulus of a casting geometry has a unit of distance (mm or m), and it is expressed as:

$$M = \frac{V}{A} \tag{1}$$

There are two main parts in a casting: **m**odulus of **c**ast **Mc** and **m**odulus of **f**eeder **Mf**. A dimensionless ratio of feeder modulus (Mf) overcasts modulus (Mc) which named as **Mfc**.

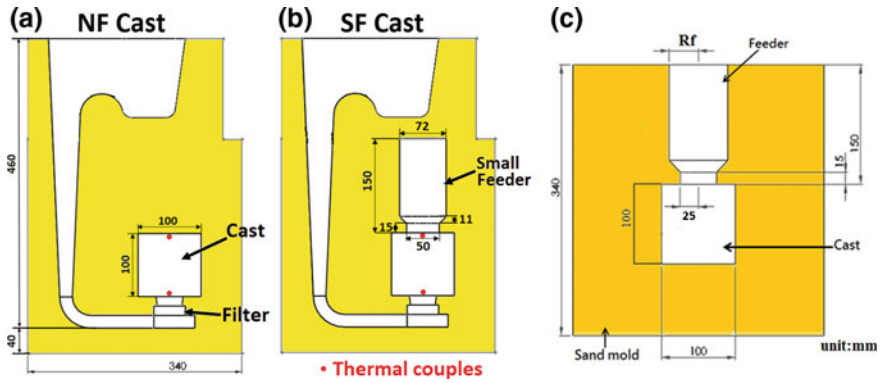

Fig. 1 Two feeding systems with the cube cast: **a** no-feeder (NF) cast, **b** small feeder (SF) cast, and **c** optimized feeder dimensions. (Noted the thermal couples located at the red points.)

Feeding Systems

In this study, a cube cast with dimensions of 100 mm × 100 mm × 100 mm (Mc = 16.67 mm) was used for this experiment. With this cast, two feeding systems and optimized feeder modeling were designed in Fig. 1. Two feeding systems are named as a **n**o-**f**eeder (NF) cast and a **s**mall **f**eeder (SF) cast (Mf = 16.97 mm). In these two runner systems, the total head height of 460 mm was designed. A pouring basin and a ceramic foam filter with dimensions of 50 mm × 50 mm 15 mm and pore size of 10 ppi were applied, in order to provide a quiescent filling and to reduce the bottom gated velocity under the critical value of 0.5 m/s [4]. To probe temperature and filling time of liquid metal into the cast, two thermal couples were attached in the gate and the top of the cast as shown in Fig. 1a, b.

Casting Experiment

To provide a rigid mold for withstanding volume expansion of the cast iron, phenolic urethane cold box (PUCB) binder was used as sand mold material. Ductile cast iron with the composition of carbon 3.5 wt%, silicon 2.25%, and sulfur 0.03% (FCD-450) was melted at 1350 ± 50°C, and it was treated with magnesium nodulant in a tundish ladle. Casting was removed from runner system. Shrinkage holes on the top of casting were sealed with paraffin wax for later Archimedes' floatation measurements. The **b**ulk **d**ensity (D_B) of the casting then can be calculated, and this measurement is correlated with the density of liquid metal as filling the casting cavity. After the D_B calculation, the castings were sectioned in halves for hardness test. Using 100 kg force and 1.588 mm hard steel sphere, Rockwell hardness was measured in every 5 mm distance within this cross section in order to visualize microstructures distributed within the center plane.

The Solidification Modeling

A **c**omputational **f**luid **d**ynamics (CFD) code, Flow-3D™ Cast v4.2 [5], has been used for this study. Two solidification models, **F**irst **P**rinciple (FP) model and **R**apid **S**olidification **S**hrinkage (RSS) model, were employed in solidification modeling.

In the RSS model, the energy equation of the metal and mold is only solved as it is considered that porosity formation is primarily influenced by metal cooling and gravity. No fluid flow and volumetric expansion are calculated in this model. The porosity volume is explicitly evaluated by the cooling rate and the density difference of the transforming from liquid to solid. In an isolated liquid region, its shrinkage volume at each time step is supplied from the liquid on its upper cells along gravity direction. Porosity is then formed on the top portions of this region as these cells begin deficit of liquid.

In the FP model, the continuity and energy equations are modified to include the volumetric source terms. In the solidification of a fluid region, a negative pressure was developed by the density difference of the liquid–solid transformation. Derived from volume loss in shrinkage, this negative pressure can be replaced by pulling the surrounding fluid. If the fluid is confined within a region, it is then built up until a critical pressure is reached. At this critical point, a macro-pore is allowed to open. The critical pressure is relative to one negative pressure to expel gases out of the liquid solution. At each time step, the complete solution of momentum and energy equations is involved in this model. The size of time step is controlled by the stability criteria associated with fluid flow.

The physical and thermal properties of ductile cast iron with carbon 3.5 wt% and silicon 2.25 wt% used in the modeling are listed in elsewhere [5]. In the solidification modeling, the bulk density (D_B) of the cast is also related to the density of liquid as filling the cavities of the cast and feeder. Therefore,

$$D_B = \frac{W_c}{V_o} = \frac{(V_o - V_s) \times \rho_M}{V_o} \tag{2}$$

where W_c is the total weight in the cast and feeder, V_o is the volume of the cast (V_c) plus the volume of feeder (V_f) if available. In the above equation, V_s is the shrinkage volume in the cast, and ρ_M is the averaged density of the solid metal predicted by the modeling at the end of the solidification. If a feeder is used on the cast, the feeder efficiency (e_f) is defined as the shrinkage volume in the feeder over the feeder volume (V_f).

$$e_f = \frac{V_s}{V_f} \times 100\% \tag{3}$$

To track the lowest position of a shrinkage macro-pore, the distance of shrinkage (Ds) is defined from the datum line at the connection point between feeder and the cast. Along gravity direction, positive distance is far from the cast while negative distance is inside of the cast.

The Feeder Modeling

Once the solidification models are approved, the validated model can be applied for feeder optimization modeling of the cube cast. In this modeling, initial liquid temperature of 1450 °C was set up at the beginning of solidification modeling. This is because approximately only 1 percent of heat loss of liquid during a very short filling time was expected [6]. To optimize a feeder, dimension of feeder radius (Rf) (i.e., Fig. 1c) is a variable in the modeling while other dimensions are fixed.

Result

Casting Experiment

Using Archimedes' method, the bulk densities (D_B) of NF and SF casts were measured and they are 6887 and 6883 (kg/m^3), respectively. Holes on top of the NF cast (Fig. 2a) and on the feeder of SF cast (Fig. 3a) are clearly observed. On the cross section, porosities (macro-pores) (e.g., Figs. 2c and 3d) are found by naked eyes. The shrinkage distances (D_S) of the NF and SF casts are, respectively, −45 and −35 (±1 mm).

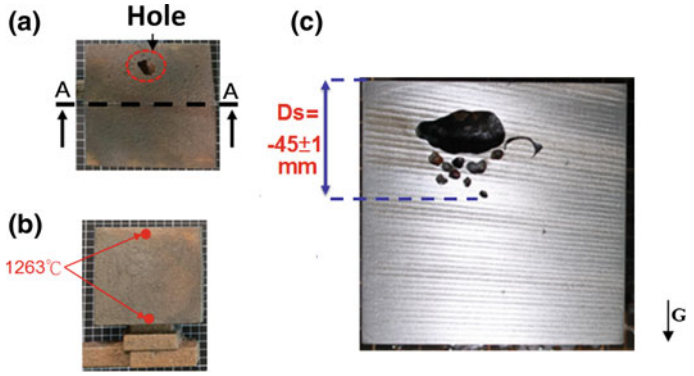

Fig. 2 Casting of the no-feeder (NF) cast in various views: **a** top, **b** front, **c** the A-A cross-sectional views

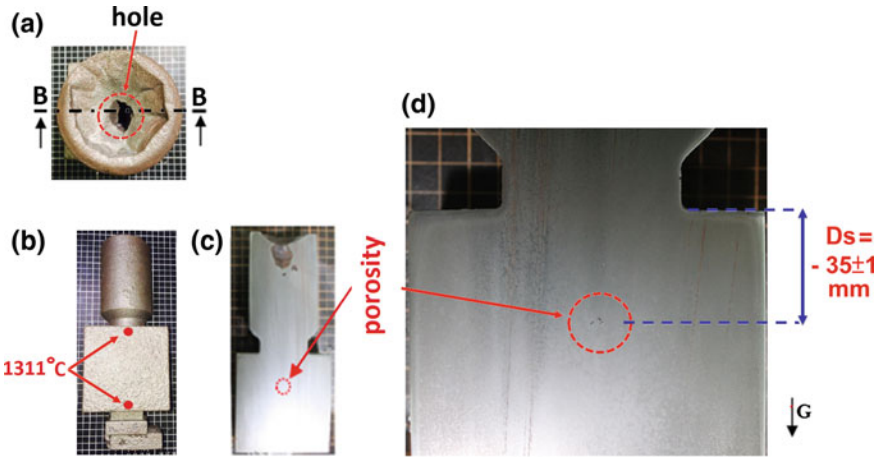

Fig. 3 Casting of the small feeder (SF) cast in various views: **a** top, **b** front, **c** the B-B cross-sectional, and **d** the magnified cross-sectional views

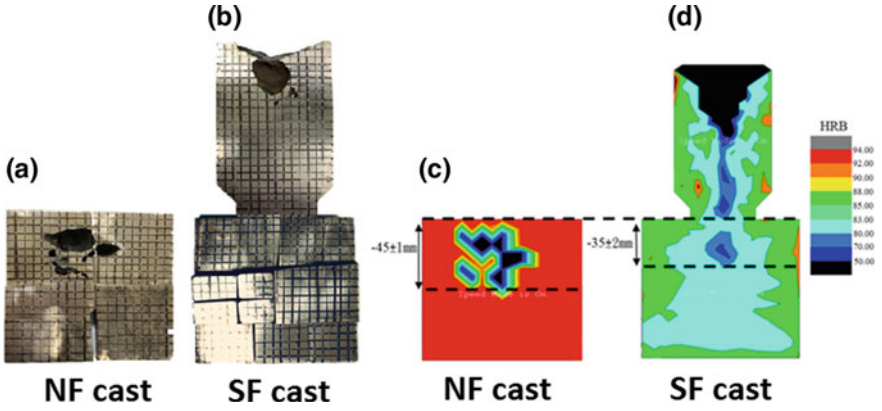

Fig. 4 Hardness measurements on the cross-sectional surfaces in the center of the **a** NF and **b** SF casts at the temperatures of 1263 °C and 1311 °C, respectively, as the filling completion, and their hardness contours plotted against to their coordinate on each cross sections of **c** NF and **d** SF casts

In hardness tests, every 5 mm distances in webs on the cross section in the center of the castings have been measured as shown in Fig. 4a, b. As these hardness measurements were plotted along the coordinates of the cross section of the casts, their hardness contours within these surfaces are illustrated in Fig. 4c, d. In these figures, the color in black is the lowest hardness (lower than 50 HRB) in the scale while the red color is the hardness greater than 92 HRB. In the porosity regions, the dark blue color is clearly displayed where the Ds of −45(±1 mm), −35(±2 mm), and −31 (±2 mm) are marked.

The Solidification Modeling

The modeling results of the casts with two different solidification models at various time frames are shown in Fig. 5. In this figure, the color in red represents regions of

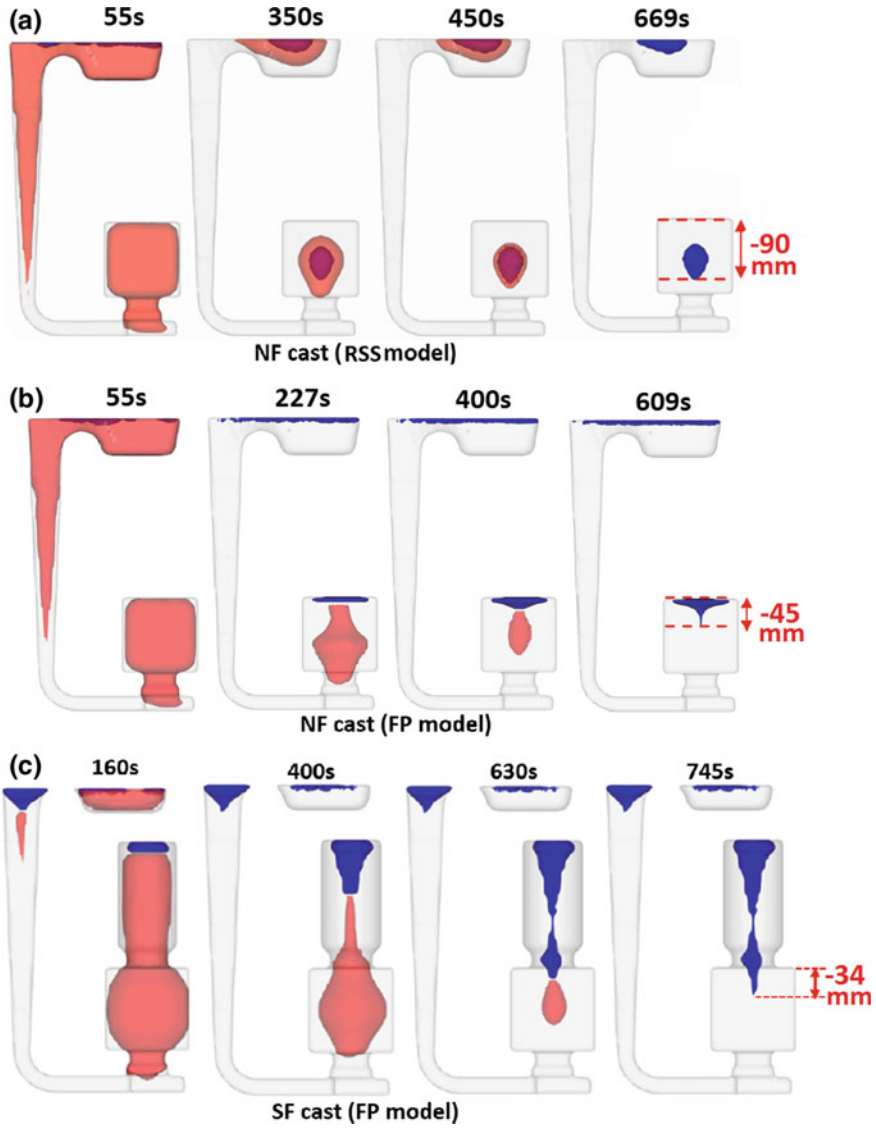

Fig. 5 Modeling results of the casts with two different solidification models: **a** NF cast (RSS model), **b** NF cast (FP model), and **c** SF cast (FP model). Noted the red religion is liquid as the blue is porosity

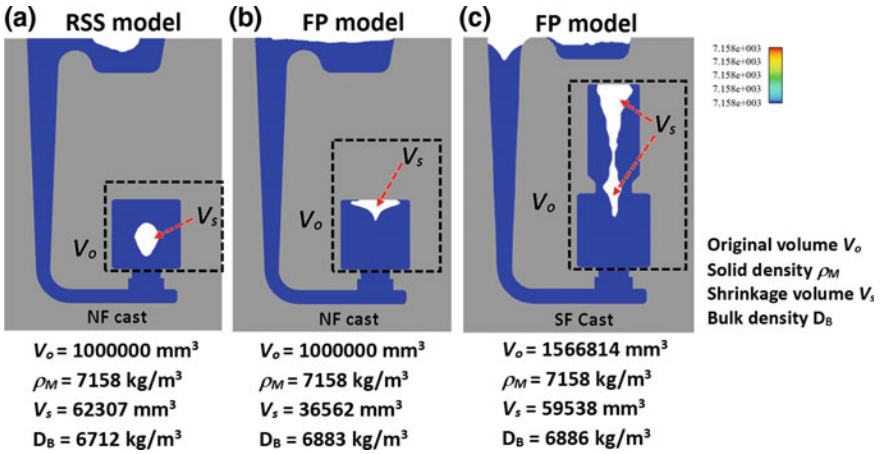

Fig. 6 Bulk density calculations by the solid density and the shrinkage volume of various casts with two different models using Eq. 2. (Noted only blue color that is 7158 kg/m^3)

liquid, while the blue color is the area of porosity (i.e., macro-pore). Also, the Ds distances of −90, −45, and −34 (mm) are measured, respectively, for the NF cast (RSS model), NF cast (FP model), and SF cast (FP model).

Using Eq. 2, the bulk densities D_B for the casts with two different solidification models are calculated as shown in Fig. 6. The uniform solid density ρ_M of 7158 kg/m^3, which is only the blue color in the contours, is presented in this figure.

The Feeder Modeling

To optimize the geometry of feeder, various feeder sizes were used for solidification modeling. Some modeling results at various modulus ratios of feeder overcast (Mfc) are shown in Fig. 7. In each modulus ratio, the shrinkage distance (Ds) and the feeder efficiency ($\boldsymbol{e_f}$) are measured at the end of solidification modeling. Against the values of Mfc, the two relationships, the ***Ds*** and the $\boldsymbol{e_f}$, are respectively presented in Fig. 8a, b.

Discussion

In the NF cast, the Ds' distances derived from the real casting (Fig. 2c), the hardness contour test (Fig. 4c) and the FP model (Fig. 5b), are all very much closed to −45 mm. The D_B measurements, obtained from the real casting and the FP model, are almost the same, and they are 6887 and 6883 kg/m^3 (Fig. 6b),

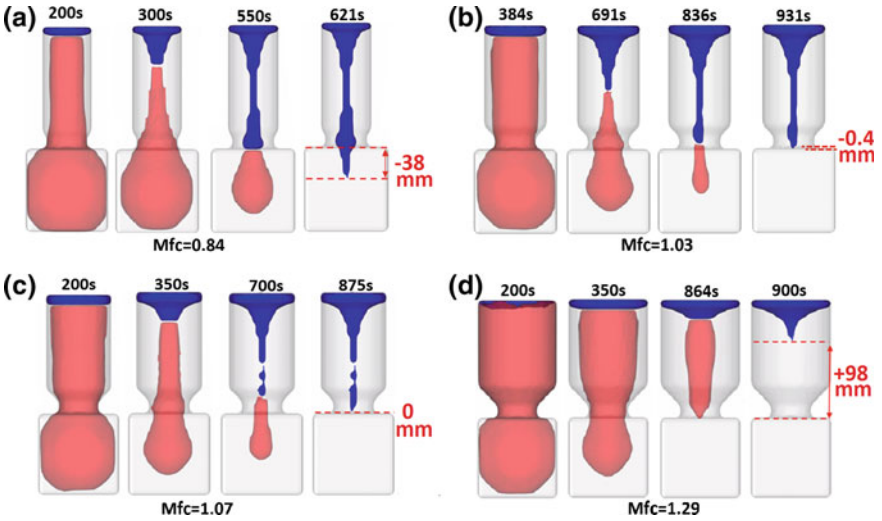

Fig. 7 Modeling results (used the FP model) at various modulus ratios of feeder overcast (Mfc): **a** Mfc = 0.84, **b** Mfc = 1.03, **c** Mfc = 1.07, **d** Mfc = 1.29. (Noted the red region is liquid as the blue is porosity.)

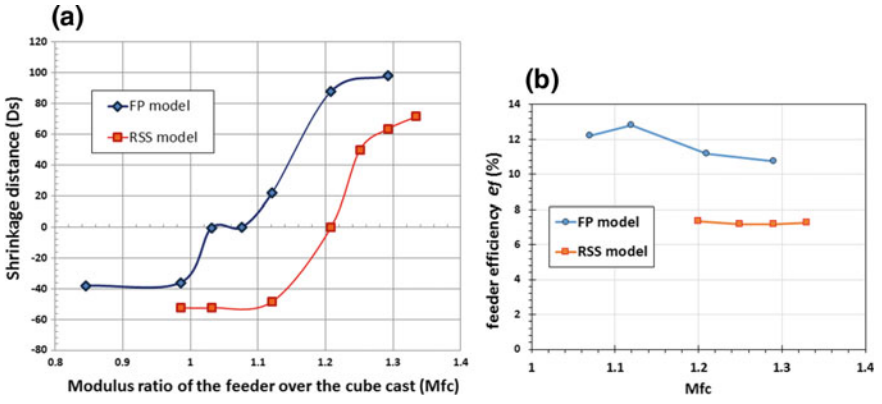

Fig. 8 Shrinkage distance and feeder efficiency plotted against to the modulus ratio Mfc in two solidification models

respectively. In contrast, the Ds (−90 mm) (i.e., Fig. 5a) and D_B (6712 kg/m^3) (i.e., Fig. 6a) values predicted by the RSS model are largely different from those in the casting. Although some shapes of the porosity predicted by the FP model are not similar to that shown in the cross section of the casting, the reverse triangle profile with its hardness lower than HRB 88 (i.e., the green color in the scale of Fig. 4c) is much correlated to a reverse conical shape of the porosity, predicted by the FP model, as sectioning in half. There is a metal skin on the top surface of the casting.

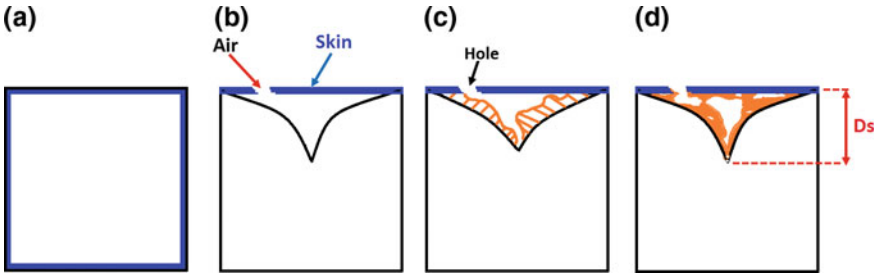

Fig. 9 Schematic of the conical cavity region, derived from the volume shrinkage at the earlier solidification process and filled with the less dense microstructures by the squeezing process due to the graphite volumetric expansion at the later solidification time

In Fig. 2a, a hole on this top skin is clearly observed and porosity is connected underneath. This top skin does not exist on the top of the conical porosity predicted by the FP modeling. The formation of this top skin is explained in Fig. 9.

Firstly, at the end of the filling process, the metal is completely full in the cavity of the NF cast (Fig. 9a). As contacting the wall of mold, the skull of liquid metal on the surface is quickly solidified since the liquid metal on surfaces losing heat into surrounding mold.

Secondly, a negative pressure is then developed due to the volume shrinkage at the liquid–solid transformation in cooling. The negative pressure is accumulated until a critical point where the atmosphere punched a hole on the top skin of the cast to release it (Fig. 9b). At this same time, a high original hydraulic pressure derived from total head height of the pouring basin is then shut by the liquid metal prematurely solidified in the spruce or in small runners. The rest of the liquid in the cast cavity becomes an isolated region without the help of this hydraulic pressure. Thus, the level of the liquid in this region starts to descend as air entering through the hole.

Thirdly, at the beginning of the solidification of ductile cast iron, the fraction of the dendrite austenite is normally 10 times larger than those of shell austenite and nodular graphite [2]. Before the solid fraction of 0.4, low density of the liquid cast iron is transformed to the high density of the austenite and the negative pressure is thus developed (Fig. 9b). Not until the solid fraction reached 0.5 or greater, the low density of nodule graphed encapsulated by austenite can grow. At this time, the remaining liquid is losing its flow fluidity within networks of solid grains. In the FP modeling, at the critical solid fraction of 0.67, above which the liquid has no fluidity, the volume expansion resulted from the nodular graphite formation is ignored.

The conical shape of the porosity in the FP model is related to the region at the solid fraction of 0.67. After this solid fraction, growing (or expanding) nodular graphite then can push the residual liquid through the inter-grains networks into the conical cavity, early developed from the volume shrinkage. This event just likes squeezing water out a porous sponge (Fig. 9c).

Finally, at each time step of growing and pushing event during the solidification proceeded, low dense microstructures with weak strength are accumulated in the conical region at the end of solidification (Fig. 9d). These weak microstructures are normally referred as micro-porosities, and they easily can be picked up by the hardness test.

The Ds distance in a casting also refers to the lowest liquid level (e.g., solid fraction of 0.65 in FP model), below which a sound microstructure can be produced, when liquid metal still has fluidity. Although the exact shape of macro-porosity cannot be predicted in the FP model, its calculation in bulk density D_B is closed to that measured by Archimedes' method. It implies that the modeling density of liquid in the cast cavity before the start of the solidification is the same as that in real casting experiment. In the FP model, the volumetric expansion at the later solidification process is ignored but the liquid metal level can be precisely located at the earlier solidification.

This FP model is efficiently enough to locate the region where sound casting structure can be produced. Also, it helps us to validate the volumetric expansion of graphite growing at the later solidification (at the solid fraction greater 0.5) correlated to the works of Fredriksson et al. [4].

In the SF casting (e.g., Fig. 3d), the Ds (i.e., −35 mm) and D_B (i.e., 6883 kg/m^3) values are closed to those (i.e., −34 mm and 6886 kg/m^3) predicted by FP modeling (Fig. 5c). The hardness contour test (Fig. 4d) is a sensitive way to reflect the variation of microstructures resulting from cooling rate. The middle blue color region (i.e., the range of HRB 70 ∼ 80) in the hardness scale in Fig. 4d is a suitable hardness range to pinpoint the macro-porosity formed before the metal has fluidity (e.g., the porosity predicted by the FP modeling, such the blue region in Fig. 5c). Near the end of solidification, such few amounts of the squeezed liquid cannot free fall by gravity or, in the other word, it cannot fill the lowest location of the porosity because it has no fluidity at this time.

Figure 8 shows the feeder optimization modeling results. In Fig. 8a, as the Ds distance is zero, the modulus ratios of Mfc are 1.07 and 1.21 from interpolating the curves predicted by the FP and RSS models, respectively. Since the FP model is more accurate to predict the Ds distance, its curve can be used to optimize feeder design. Against to the same ratio Mfc (i.e., 1.07) found in zero Ds distance, the feeder efficiency ***ef*** (i.e., 12.2%) can be derived from the FP modeling curve in Fig. 8b. This feeder with a high feeder efficiency and a minimum size is recommended for future usage in feeding ductile cast iron.

In the FP modeling curve in Fig. 8a, a plateau in the range between 1.03 and 1.07 of Mfc ratio is closed to the Ds of zero. This abrupt transforming curve is an evidence of that the FP model considers the volumetric expansion of spheroidal graphite growing while the RSS model does not. In the FP modeling, as Mfc is 1.07, the residual liquid with volume of 2089.0 mm^3 is remained within the cast (e.g., at 700 s in Fig. 7c). The last residual liquid is eventually transformed to eutectic structure of nodular graphite and shell austenite without creating any porosity inside of the cast. That is Ds of zero.

Conclusion

1. The shrinkage distance Ds distance predicted by the first principle modeling is an accurate measuring method to locate the lowest liquid level where macro-porosity is formed.
2. A large volumetric expansion by growing spheroidal graphite at solid fraction greater than 0.5 has been validated by the different results found between the FP modeling and real casting. Conical shape of the porosity in the FP model is related to the region at the solid fraction of 0.67.
3. For a cube cast with Mc of 16.67 mm, the optimized feeder, which is a minimum size (i.e., Mf = 17.84 mm or Mfc = 1.07) and a large feeder efficiency (12.2%), can be proposed.
4. In the diagram of the Ds distance plotted against to the Mfc ratio, the plateau in the FP modeling curve is an evidence of that the FP model considers the volumetric expansion of spheroidal graphite growing.

Acknowledgements The authors personally acknowledge the help of the colleagues in Shou Chen Industry Co., Ltd No. 168, Deli Rd., Taiping District, Taichung City 411, Taiwan (R.O.C.), for casting experiments.

References

1. Campbell J (2011) Complete casting handbook, metal casting process, metallurgy, techniques and design, first edition, pp 347–352 [1a], p 406 [1b], p 663 [1c], p 666 [1d]
2. Fredriksson H, Stjerndahl J, Tinoco J (2005) On the solidification of nodular cast iron and its relation to the expansion and contraction. Mater Sci Eng, A 413–414:363–372
3. Schmidt WA, Sullivan E, Taylor HF (1954) AFS Trans 9:70
4. Hsu F-Y, Lin H-J (2011) Foam filters used in gravity casting. Metall Mater Trans B 42 (6):1110–1117
5. Flow 3D Casts, Flow Science. https://www.flowsciences.com/2018.06
6. Richins DS, Wetmore WO (1952) Hydraulics applied to molten aluminum. Trans ASME, 725–732